International Journal Of Industrial Electronics Control and Optimization
Print ISSN: 3517-2645
Online ISSN: 3568-2645
Homepage: https://ieco.usb.ac.ir/

An Effective Damping Control Approach in Grid-Connected Converters

Anwer J. Ali[1] | Sirwan Shazdeh[1] | Hassan Bevrani[1] | Rahmatollah Mirzaei[1] | Qobad Shafiee[1] |

Smart/Micro Grids Research Center (SMGRC), University of Kurdistan, Sanandaj, Iran.[1]
Corresponding author's email: a.jalalali@uok.ac.ir.

Article Info

Article type:
Research Article

Article history:
Received: 24- July -2023
Received in revised form: 15- October -2023
Accepted: 04- November -2023
Published online: 26- November -2023

Keywords:
grid connected converters, virtual synchronous generator, swing equation, damping control.

ABSTRACT

The primary objective of this paper is to address the adverse effects of active power fluctuations on grid-connected converters. One of the challenges in integrating high levels of solar photovoltaic power into the utility grid is the lack of inertia from converter-based resources. This paper proposes a solution to this challenge by synthesizing additional inertia and damping properties using power electronics converters. They emulate the inertia and damping properties of synchronous generators. The paper discusses different approaches to achieving effective damping control in grid-connected converters. It proposes a genetic algorithm optimization tool to optimize virtual damping and inertia parameters. The goal is to suppress oscillations and ensure stable grid operation. The proposed method is evaluated in both time-domain and frequency-domain analyses. The simulation results demonstrate the validity of the optimization technique and implementation procedure. Using virtual inertia and damping properties ensures stable grid operation and improves the integration of solar photovoltaic power into the utility grid. The paper provides a detailed discussion of the approach, optimization tool, and simulation results, highlighting the effectiveness of the proposed method.

I. Introduction

In the global energy market, renewable energy sources such as solar systems are increasingly considered as viable alternatives to conventional sources of energy for power generation. The growing demand for energy and the environmental concerns associated with fossil fuels are the main reason for this revolution in energy production [1]. The integration of PV power into the utility grid has become a significant area of research and has garnered substantial public attention [2]. This interest is fueled by the decreasing costs of solar PV panels and the fast growth of related technologies [3]. In PV systems, converters are commonly used as interfaces between the PV arrays and the grid. However, converter-based resources (CBRs) introduce zero/low inertia dynamics into the grid due to the absence of rotating masses, which typically serve as sources of inertia. As a result, the overall inertia of the integrated power system is reduced due to the high penetration of CBRs [4]. To address this challenge and enhance power system stability with high PV penetration, the synthesis additional inertia and damping properties virtually has emerged as a promising solution [5].

Power electronic converters, equipped with short-term energy storage and appropriate control mechanisms, can be employed to emulate inertia and damping properties within the power system, thereby ensuring stable grid operation [6]. Unlike an actual synchronous generator (SG), the dynamic response of the system can be improved by manipulating the parameters of a virtual dynamic system. In addition to the virtual inertia control [7], other SG dynamics can be emulated on the converter control which is known as virtual synchronous machine (VSM) [8], [9], virtual synchronous generator (VSG) [10], [11], or synchronverter [12], [13].

Grid-connected converters (GCCs) with dynamic characteristics emulation features have gained significant interest on a global scale, as they offer power systems with desirable dynamics. GCCs possessing these properties are referred to as grid-forming converters [14]. It is important to note that the term “grid-forming” can be used to describe voltage and frequency control as a voltage source converter, and it can operate in both grid-connected and islanded scenarios [15]. For the sake of simplicity, the term "GCC" instead of “grid-forming GCC” will be used throughout the rest of this paper. GCCs play a crucial role in the future power grids due to the advancement of renewable energy generation. Since GCCs lack a rotating mass to provide inertia support for the grid, a virtual governor droop characteristic is employed to automatically track frequency changes, and a damping property is incorporated to mitigate undesirable oscillations [16]. Thus, the concept of VSG control, which emulates the swing equation of a synchronous generator to provide inertia and damping support for the power grid, offers a viable solution [17]. As a result, a new type of grid-forming control with an enhanced P-ω control loop is implemented. In recent years, various methods for emulating the swing equation with different damping techniques have been proposed [14], [18].

Despite sharing similar foundational principles, the control strategies employed in GCCs exhibit significant differences, leading to various approaches for achieving inertia and damping effects [19]. While the differential swing equation of SGs is commonly utilized to emulate inertia, alternative methods have been explored for virtual damping. Early studies in the literature focused on damping-free (DF) GCC control [11], [12]. Subsequent investigations introduced different techniques to enhance the GCC control structure, such as virtual damper windings (VDW) [20], [21], damping correction loops (DCL) [22], state feedback (SF)[23], and low-pass filtered state feedback (LPFSF) [24]. Additional damping techniques have been proposed, including the use of virtual power system stabilizers, artificial intelligence-based methods [25], output reactance boosting through virtual impedance control [26], fuzzy control strategies[27]. These approaches offer a broader range of options for achieving effective damping control in GCCs. Parameter-based approaches with self-adaptation have shown promising potential in enhancing the dynamic responses of active power and/or frequency by appropriately tuning the parameters in the VSG. [28]. These approaches encompass various techniques, including the incorporation of virtual inertia [29], [30], adjustment of damping factor [31], and simultaneous optimization of both parameters [32]–[34]. In [9], an effective damping method to improve VSM responses is proposed, while the stability of the DC-link voltage is not considered. The study in [28] presents a simple improved virtual inertia strategy based on a differential compensation model, addressing the issue of governor removal. Meanwhile, [29] introduces an approach to enhance oscillation damping and increase power system stability, but lacks a detailed consideration of certain parameters like the inertia coefficient. Additionally, the authors of [30] propose an adaptive virtual inertia control strategy, acknowledging its potential to improve the frequency response, but highlighting the need for optimization.

In this paper, the primary objective is to mitigate the adverse active power fluctuations observed at the output of a typical GCC. Therefore, the contributions of this paper can be summarized as follows:

- The implementation of a virtual dynamic loop that includes damping and inertia to suppress oscillations and ensure proper coordination between virtual damping and virtual inertia.
- The use of a genetic algorithm optimization tool to optimize both damping and inertia parameters. This method offers a simple and accurate approach to fine-tuning the control parameters, leading to improved system response and performance.
- comprehensive analysis in both the time-domain and frequency-domain, include examining step response characteristics and pole locations, providing insights into the system's stability and dynamic behavior.

Briefly, this paper contributes to the understanding of how to mitigate active power fluctuations in GCCs using a virtual dynamic loop with optimized virtual damping and virtual inertia parameters, and provides a method for evaluating the effectiveness of this approach.

The remaining sections of the paper are organized as follows: Section 2 provides an overview of the grid-forming converter concept. The operation principles of GCCs are explained in detail in Section 3. In Section 4, a proper linear dynamic model for active power and frequency response, as well as damping control synthesis, is presented. Section 5 explains the proposed design methodology for parameter optimization. Simulation results and discussion are presented in Section 6. Finally, the paper is concluded in Section 7.

II. Concept and Structure of GCCs

Based on their control strategies, Grid-connected converters can be classified into two primary topologies: grid-following and grid-forming [35], [36]. A grid-following converter uses a Phase-Locked Loop (PLL) and current loop to achieve rapid control of the converter's output current. The output characteristic of a grid-following converter can be visualized as an ideal AC current source connected in parallel with an admittance associated with the grid. Fig. 1(a) depicts a simplified equivalent model of this configuration.

In contrast, grid-forming converters regulate the output active and reactive power by controlling the voltage magnitude and frequency. They can be represented as an ideal AC voltage source connected in series with impedance. The simplified equivalent model of a grid-forming converter is illustrated in Fig. 1(b). GCCs have the capability to adjust their output power to accommodate loads and maintain local voltage and frequency at desired levels, even in unexpected scenarios. One notable advantage of dynamic characteristic-based GCCs is their rapid response to changes in output power and frequency. Unlike SGs, the transition time between such changes is significantly reduced in GCCs. This enhanced response enables GCCs to adapt to various conditions and react more efficiently compared to SGs. Although grid-following converters can regulate the output of real and reactive power by injecting a current with a specific phase angle, they do not have direct control over system voltage and frequency. In grid-following converters, the voltage and frequency references are typically provided externally, either by a GCC or the connected power grid.

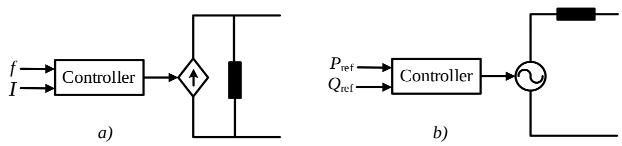

Fig. 1. Simplified equivalent models of power converters: (a) grid-following converter, (b) grid-forming converter.

Fig. 2 depicts a simplified control system of a GCC, comprising two primary subsystems: a voltage controller and a dynamic characteristic emulator unit. These subsystems provide the main reference signals to the voltage controller. The dynamic characteristic emulator unit consists of a control mechanism designed to replicate the necessary dynamics, allowing it to fulfill various functions such as virtual damping control, droop control, VSG, or any other desired dynamic behavior [19].

To accomplish dynamic characteristic emulation in GCCs, the control system incorporates several blocks. Fig. 3 illustrates a representative GCC along with its detailed control system. The "P-droop, inertia, and damping emulator" block is the core of the GCC control system, responsible for emulating the desired droop characteristics, inertia, and damping effects. Another critical block is the "output impedance emulator" which applies a virtual impedance control loop to enable the GCC to exhibit an equivalent output impedance characteristic.

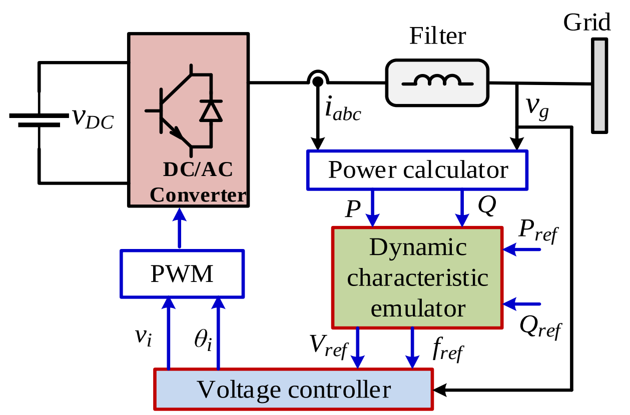

Fig. 2. Simplified GCC structure.

the "Q-droop emulator" block is also crucial in the dynamic characteristic emulation system of GCCs. It enables the implementation of the droop relationship between voltage and reactive power, ensuring that the reactive power output of the GCC follows the desired droop characteristics. This block plays a significant role in maintaining proper voltage regulation and reactive power support within the power system. Collectively, these blocks enable the GCC to exhibit the desired control behaviors and characteristics [26].

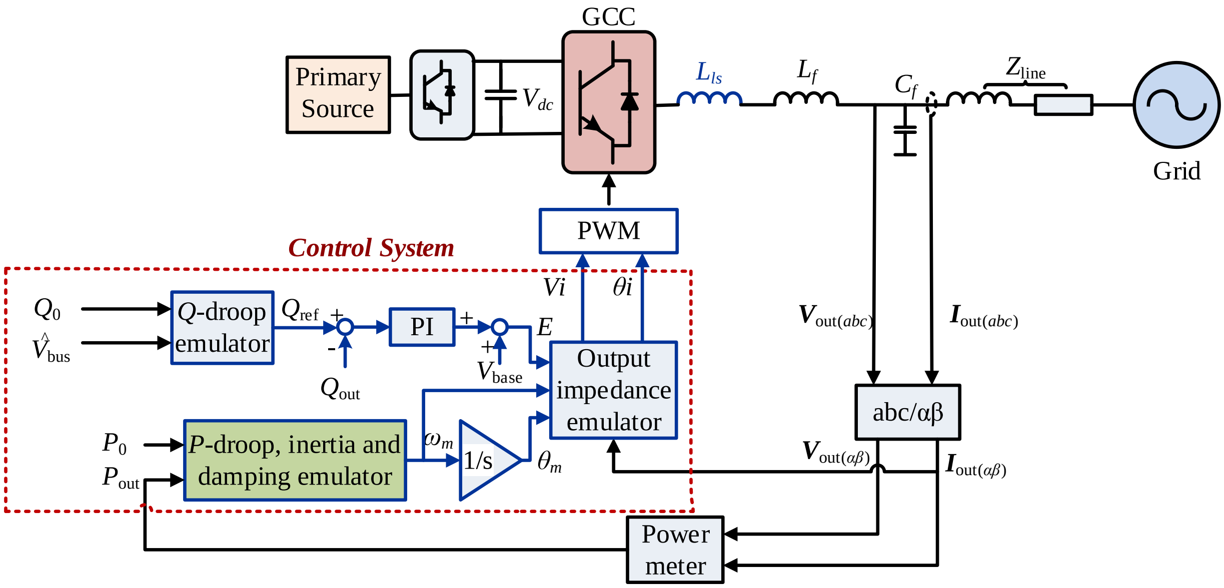

Fig. 3. Basic control structure of a grid-forming GCC.

III. Operation Principles of GCCs

In a GCC, the swing equation of SG can be emulated using a power controller. This emulation enables the implementation of frequency droop, power-oscillation damping, and/or virtual inertia characteristics [37]. A comprehensive control scheme for a VSG that incorporates virtual inertia control, droop control, and damping control can be represented mathematically as [18]

$$P_{out} - P_0 = J\omega_0 \frac{d\omega_m}{dt} + k_p(\omega_m - \omega_0) + D(\omega_m - \omega_g) \tag{1}$$

where P_0 denotes the reference power determined by the governor, P_{out} represents the measured output power, J is the moment of inertia, D is the damping factor, ω_m represents the rotor angular frequency, ω_g represents the angular frequency of the grid where the voltage sensor is installed, k_p is the droop coefficient, and ω_0 represents the nominal angular frequency.

The angular momentum (M) can be expressed as the product of the moment of inertia (J) and the angular synchronous velocity (ω_0). Hence, (1) can be modified as follows:

$$P_{out} - P_0 = M \frac{d\omega_m}{dt} + k_p(\omega_m - \omega_0) + D(\omega_m - \omega_g) \tag{2}$$

Since it can be challenging to measure ω_g directly, it is commonly approximated by $\tilde{\omega}_g$, which represents the angular frequency estimated through the use of a PLL with the output voltage V_{out} [18] .Fig. 4(a) illustrates this process.

The Non-PLL method has emerged as the preferred choice for damping control over the PLL-based method. Among the various techniques, the Non-PLL method has gained popularity and is illustrated in the block diagram shown in Fig. 4(b). The primary difference between the PLL-based and Non-PLL damping techniques lies in the way damping power is generated. In the Non-PLL approach, damping power is derived using the nominal frequency rather than the grid frequency [38]. Consequently, equation (2) can be modified as follows:

$$P_{out} - P_0 = M \frac{d\omega_m}{dt} + k_p(\omega_m - \omega_0) + D(\omega_m - \omega_0) \tag{3}$$

As per the given information, the mathematical expressions for droop control and damping power, as described in equation (3), are identical. This suggests that the droop coefficient and damping factor are equivalent and serve the same purpose within the control loop. The damping factor is intended to mitigate oscillation modes within the control system, while the droop coefficient is responsible for maintaining the required frequency levels in power systems and ensuring the proper distribution of power among converters in a proportional manner [28].

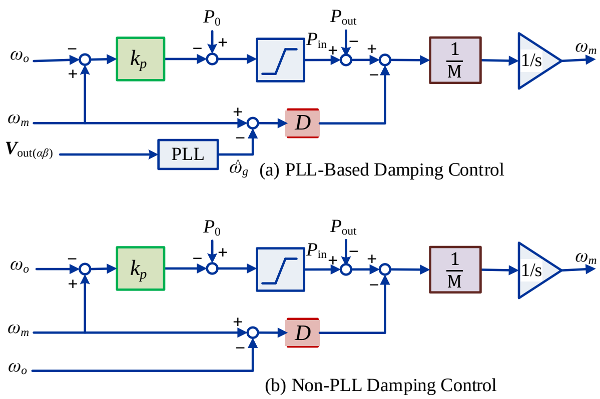

Fig. 4. Swing Equation emulation of GCC using traditional damping control. (a) PLL-based damping control. (b) Non-PLL damping control.

IV. Dynamic expressions

This section outlines a basic dynamic model that describes the active power-frequency response of the GCC. This model is essential for designing damping control strategies. Fig. 5 depicts a simplified diagram of the GCC system.

The synchronizing power coefficient K_s of the GCC is commonly represented as follows [24]:

$$K_s = \frac{\partial P_{out}}{\partial \delta} \approx \frac{EV_g cos\delta_0}{X_T} \approx \frac{V_{base}^2\sqrt{1 - X_T^{*2}}}{X_T} \quad (4)$$

where, E represents the electromotive force, V_g denotes the grid voltage, V_{base} represents the rated voltage, S_{base} is the rated power, and X_T^* denotes the per unit value of total reactance as depicted in Fig. 5.

The derivative of the power angle δ can be expressed as

$$\frac{d\delta}{dt} = \left(\omega_m - \omega_g\right) \quad (5)$$

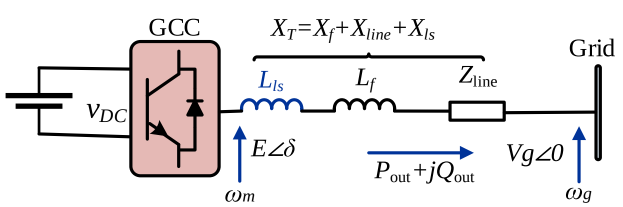

Fig. 5. Simplified diagram of a grid-connected GCC.

The GCC closed-loop transfer functions of the active power, and frequency related to the input active power (ΔP_0) and disturbance input grid frequency $(\Delta\omega_g)$ can be obtained by deriving (3) to (5). The resulting expressions are given by (6) to (9). It should be noted that the dynamics of the PLL are disregarded. Consequently, the GCC system will be a typical second-order system, and both the PLL-based and Non-PLL systems exhibit identical characteristics.

$$\frac{\Delta P_{out}}{\Delta P_0} = \frac{K_s}{Ms^2 + \left(k_p + D\right)s + K_s} \quad (6)$$

$$\frac{\Delta\omega_m}{\Delta P_0} = \frac{s}{Ms^2 + \left(k_p + D\right)s + K_s} \quad (7)$$

$$\frac{\Delta P_{out}}{\Delta\omega_g} = \frac{K_s k_p + K_s Ms}{Ms^2 + \left(k_p + D\right)s + K_s} \quad (8)$$

$$\frac{\Delta\omega_m}{\Delta\omega_g} = \frac{K_s + ds}{Ms^2 + \left(k_p + D\right)s + K_s} \quad (9)$$

The characteristic equations of (6)-(9) is

$$Ms^2 + \left(k_p + D\right)s + K_s = 0 \quad (10)$$

Thus, the undamped natural frequency (ω_n) and the damping ratio (ζ) can be found as

$$\omega_n = \sqrt{\frac{K_s}{M}} \quad (11)$$

$$\zeta = \frac{k_p + D}{2\sqrt{MK_s}} \quad (12)$$

The transient response performance of a control system can be assessed by parameters such as overshoot, rise time, delay time, and settling time. The natural frequency, ω_n, directly influences the rise time, delay time, and settling time, but it does not affect the overshoot. On the other hand, the maximum overshoot is solely dependent on the damping ratio, ζ, and can be controlled independently. Consequently, in practice, the settling time can be reduced by increasing ω_n while keeping ζ constant. For 0.7< ζ <1, the step response is oscillatory, but the oscillations are well-damped and are hardly perceptible [39], [40].

V. Proposed Method for Parameters Optimization

Parameter-based techniques with self-adaptation possess the capability to enhance the dynamic responses of active power and/or frequency by effectively adjusting the parameters within the VSG. By appropriately tuning these parameters, the dynamic behavior of the VSG can be optimized, leading to improved performance in terms of active power and frequency control.

There are numerous techniques available for finding optimal solutions that can work efficiently, including artificial intelligence, neural networks, fuzzy systems, and soft computing. Among these techniques, the Genetic Algorithm (GA) stands out as a robust method that consistently produces the best possible solutions for optimization [41]. The GA is well-suited for solving numerous practical optimum design problems that are characterized by a combination of continuous and discrete variables, as well as discontinuous and nonconvex design spaces, which cannot be effectively addressed using standard nonlinear programming techniques [42]. Consequently, the GA is considered an optimal choice for optimization.

In this study, the optimal values of M and D (M^* and D^*) are obtained for different scenarios through the implementation of the GA using MATLAB codes. Subsequently, the performance and stability of the system are analyzed. The proposed method of using the GA optimization tool to optimize virtual damping and virtual inertia parameters in GCCs has moderate computational complexity.

The important key points of the GA process of obtaining M^* and D^*, include; the cost-function (or objective function), M and D variation bounds, and the desired prescribed performance.

The cost-function (*cf*) is defined based on the settling time (t_s) and Maximum overshoot (M_p) tolerances as

$$cf = \left(t_{s_{Desired}} - t_{s_{Actual}}\right)^2 + \left(M_{p_{Desired}} - M_{p_{Actual}}\right)^2 \qquad (13)$$

where, $t_{s_{Desired}}$ is the desired settling time that can be calculated as,

$$t_{s_{Desired}} = \frac{4}{\zeta\omega_n} \qquad (14)$$

$t_{s_{Actual}}$ is the actual settling time measured from the step response of the system,

$M_{p_{Desired}}$ is the desired overshoot indicated based on the desired ζ, as

$$M_{p_{Desired}} = e^{-\left(\frac{\zeta}{\sqrt{1-\zeta^2}}\right)\pi} \qquad (15)$$

and $M_{p_{Actual}}$ is the actual overshoot measured from the step response of the system.

The optimal values can be obtained based on the minimization of the objective function. The flow chat of the GA based optimization algorithm is illustrated in Fig. 6.

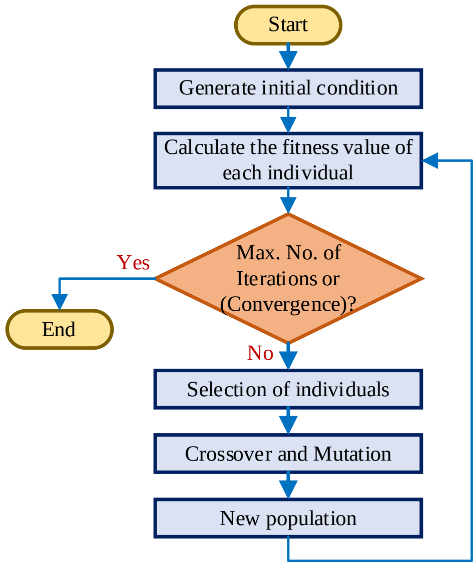

Fig. 6. Flowchart of the GA optimization algorithm.

VI. Simulation Results and Discussion

In Table 1, the control parameters of the GCC are considered and designed. Notably, the per unit values of the parameters are defined such as ratios relative to a specified base value as.

$$k_p{}^* = k_p \frac{\omega_0}{S_{base}}, and\ X_T{}^* = X_T \frac{S_{base}}{V_{base}^2}$$

TABLE 1
GCC's PARAMETERS

Parameter	Value	Parameter	Value
V_{base}	200 V	$P_0{}^*$	1 pu
S_{base}	5 kVA	$X_T{}^*$	0.3 pu
ω_0	377 rad/s	$k_p{}^*$	20 pu

The primary objective of this design is to enhance damping. Therefore, an overshoot value of 0.0015, which corresponds to a damping ratio of ζ =0.9, is selected. Different settling times and, consequently, different pole locations are considered. The obtained optimized results are presented in Table 2.

TABLE 2
SYSTEM BEHAVIOR WITH OPTIMAL VALUES OF D AND M

Case	Desired t_s(s)	Desired M_p	Desired ζ	D^*	M^*
1	0.2	0.0015	0.9	1.19	0.041
2	0.3	0.0015	0.9	1.7	0.075
3	0.4	0.0015	0.9	2	0.1
4	0.5	0.0015	0.9	2.42	0.14

The corresponding step response and pole locations of the system depicted by (6) can be observed in Figs. 7 and 8 respectively.

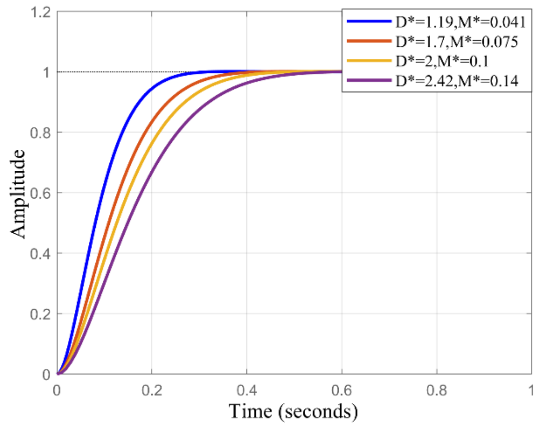

Fig. 7. Step responses of the GCC with damping.

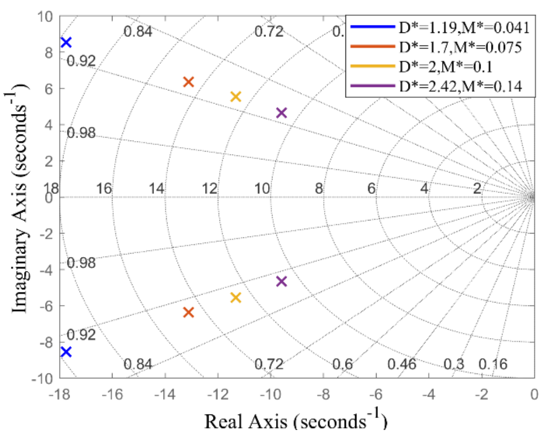

Fig. 8. Pole locations of the GCC with damping.

When the damping coefficient D is disregarded (D = 0), the system depicted by (6) become oscillatory and the system parameters are changed accordingly to the new values given in Table 3, with the same previous values of M*.

The corresponding step response and pole locations of the system can be found in Figs. 9 and 10 respectively. The comparative pole locations of the system with and without damping is illustrated in Fig. 11.

TABLE 3

THE SYSTEM'S BEHAVIOR WITH D=0.

Case	Actual t_s(s)	Actual M_p	D	M^*
1	1.1678	0.5895	0	0.041
2	2.1981	0.6806	0	0.075
3	2.8111	0.7171	0	0.1
4	3.9136	0.7554	0	0.14

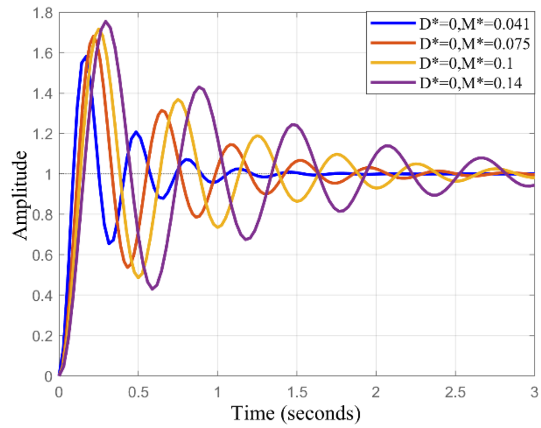

Fig. 9. Step response of the GCC without damping.

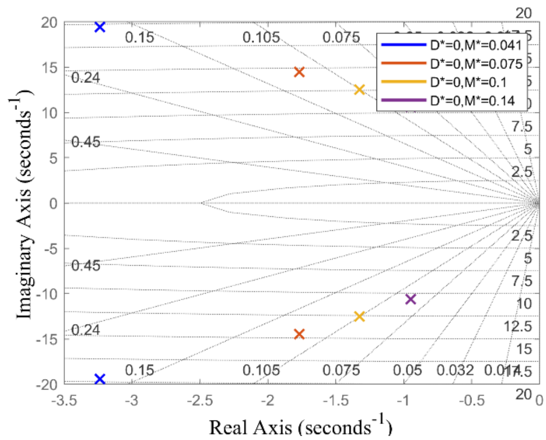

Fig. 10. Pole locations of the GCC without damping.

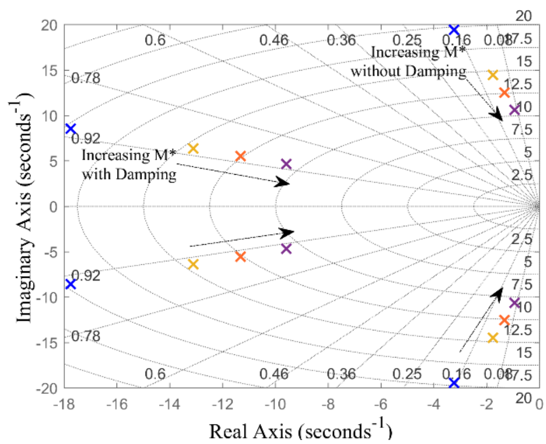

Fig. 11. Pole locations of the GCC with and without damping.

To further highlight the effect of the damping term on the system, the comparative step response and pole locations of the GCC system depicted by (6) to (9) are provided in Figs. 12, 13 and 14, respectively, when D^*=1.19 and M^*=0.041 with damping, and D=0 and M^*=0.041 without damping.

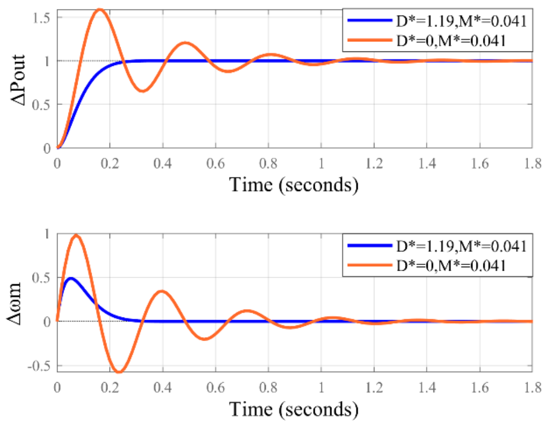

Fig. 12. Step response of the GCC with and without damping related to the set input active power (ΔP_0).

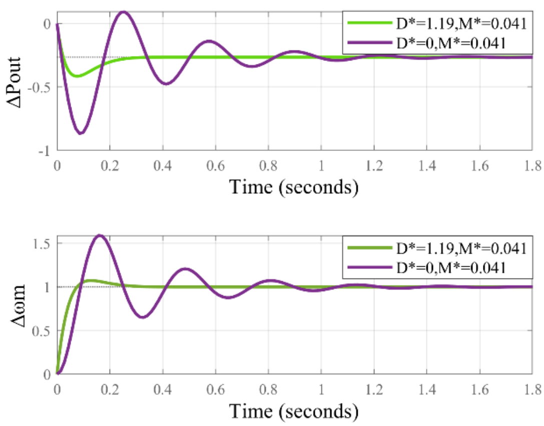

Fig. 13. Step response of the GCC with and without damping related to disturbance input grid frequency ($\Delta\omega_g$).

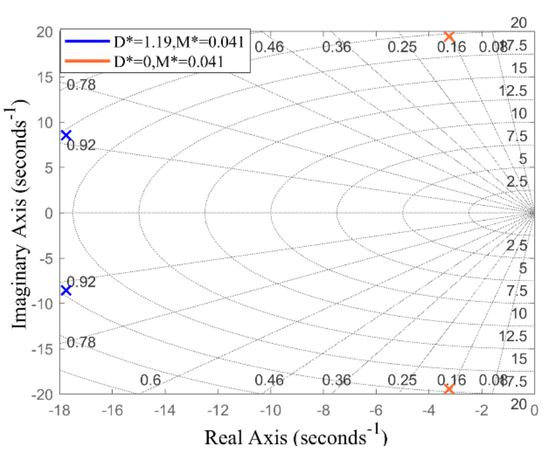

Fig. 14. Pole locations of the GCC with and without damping.

The system is tested again with the optimal values of M* and D*, when ζ changing from 0.7 to 1 and t_s =0.4 s. the obtained results are given in table 4. The corresponding system responses are shown in Figs.15 and 16 respectively.

TABLE 4
THE SYSTEM'S BEHAVIOR WHEN ζ CHANGING FROM 0.7 TO 1 AND T_S=0.4S.

Case	Desired t_s(s)	Desired M_p	Desired ζ	D^*	M^*
1	0.4	0.046	0.7	1.5	0.1
2	0.4	0.0152	0.8	1.75	0.1
3	0.4	0.0015	0.9	2	0.1
4	0.4	0	1	2.42	0.1

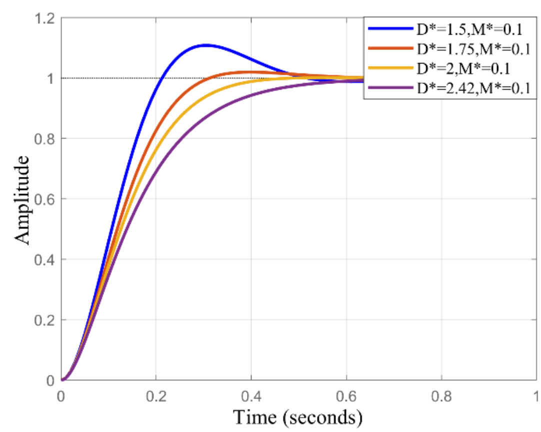

Fig. 15. Step response of the GCC with damping when ζ changing from 0.7 to 1.

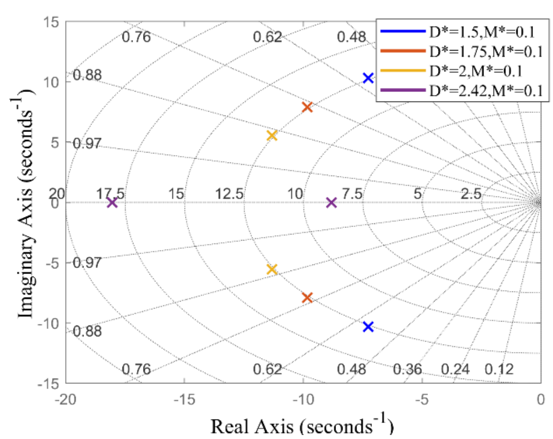

Fig. 16. Pole locations of the GCC with damping when ζ changing from 0.7 to 1.

These simulation results illustrate the step response and pole locations of the GCC under different damping conditions, highlighting the impact of damping on the system's behavior and stability. They also depict the importance of properly tuning and optimizing the GCC parameters. The performance improvement can be easily discerned from the step response, which shows a shorter settling time and decreased overshoot, while the poles settle at more stable positions.

To verify the effectiveness of the proposed optimal damping control design method, simulations were conducted in the MATLAB/Simulink environment. Fig. 17 provides an overview of the case study, serving as the simulation setup. The circuit parameters are displayed in Fig. 17, and additional system parameters can be found in Table 1. Fig. 18 presents the simulation results, illustrating the GCC output power and frequency fluctuations in two scenarios: with the optimal damping control loop and without damping control. It is evident that the desired performance can be achieved with the optimal damping control loop, in contrast to the case where no damping characteristics are present. These findings support the effectiveness of the proposed optimal damping control design method.

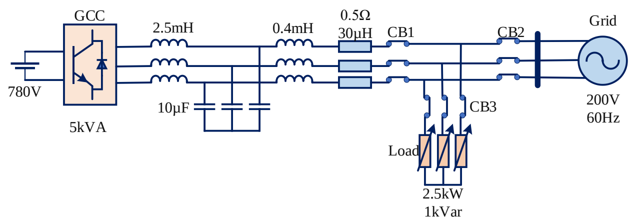

Fig. 17. The schematic of a grid-connected GCC case study in MATLAB/Simulink environment.

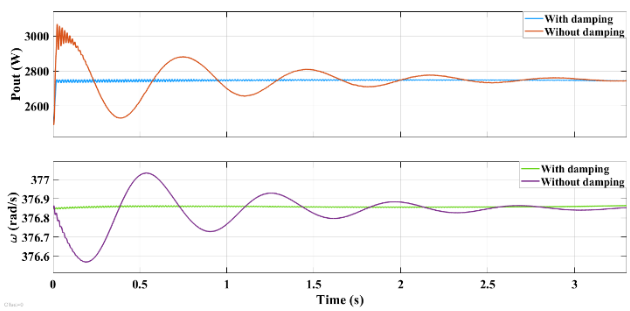

Fig. 18. The GCC output power and frequency in grid connected mode.

Since the proposed method is performance-index based, to compare its dynamic performance with existing methods, similar analyses to (6) are applied to the following methods. The performance indices for this comparative study are shown in Table 5. It is important to note that a large inertia is desired for better inertia support. However, insufficient damping can lead to significant oscillations and overshoot, which may damage the GCC, as demonstrated in the DF method. On the contrary, the VDE methods exhibit good damping ability. As mentioned earlier, the VDE methods can provide better dynamic responses if their parameters are properly chosen, as we have done in our optimization approach. The effectiveness of the proposed approach can be clearly observed by demonstrating better dynamic performance, such as shorter rising (t_r) and settling times (t_s) or overshoot (M_p), compared to other methods given in [11], [20], [22], [23] and summarized in [24].

TABLE 5
COMPARISON OF THE PERFORMANCE INDICES OF DYNAMIC RESPONSES.

DF			Proposed method				
t_r(s)	t_s(s)	M_p	t_r(s)	t_s(s)	M_p	D^*	M^*
0.0922	3.12	0.724	0.0898	2.811	0.71713	0	0.1
VDE			Proposed method				
t_r(s)	t_s(s)	M_p	t_r(s)	t_s(s)	M_p	D^*	M^*
0.236	0.384	0.00152	0.2287	0.372	0.001503	2	0.1
DCL			Proposed method				
t_r(s)	t_s(s)	M_p	t_r(s)	t_s(s)	M_p	D^*	M^*
0.236	0.386	0.00152	0.2427	0.395	0.001534	2.143	0.112
SF			Proposed method				
t_r(s)	t_s(s)	M_p	t_r(s)	t_s(s)	M_p	D^*	M^*
0.166	0.263	0.00537	0.1601	0.252	0.005342	1.352	0.056
LPFSF			Proposed method				
t_r(s)	t_s(s)	M_p	t_r(s)	t_s(s)	M_p	D^*	M^*
0.162	0.254	0.00603	0.1582	0.248	0.006101	1.337	0.055

VII. Conclusion

This paper proposes a solution of synthesizing additional inertia and damping properties virtually using power electronic converters. The paper explores different approaches to achieve effective damping control in GCCs and proposes a genetic algorithm optimization tool to optimize virtual damping and virtual inertia parameters. The primary objective of the paper is to mitigate adverse active power fluctuations in GCCs. The proposed method is evaluated in both the time-domain and frequency-domain analyses. Overall, the proposed method uses virtual inertia and damping properties to ensure stable grid operation and improve the integration of solar PV power into the utility grid. The simulation results emphasize the validity of the optimization technique and implementation procedure.

References

[1] S.-J. Yoon and K.-H. Kim, "Harmonic Suppression and Stability Enhancement of a Voltage Sensorless Current Controller for a Grid-Connected Inverter Under Weak Grid," *IEEE Access*, vol. 10, pp. 38575–38589, 2022, doi: 10.1109/ACCESS.2022.3166592.

[2] Y. Tu, J. Liu, T. Liu, and X. Cheng, "Impedance-Based Stability Analysis of Large-Scale PV Station under Weak Grid Condition Considering Solar Radiation Fluctuation," in *2018 International Power Electronics Conference (IPEC-Niigata 2018*

-ECCE Asia)*, 2018, pp. 3934–3939. doi: 10.23919/IPEC.2018.8507415.

[3] M. M. Gulzar, A. Iqbal, D. Sibtain, and M. Khalid, "An Innovative Converterless Solar PV Control Strategy for a Grid Connected Hybrid PV/Wind/Fuel-Cell System Coupled With Battery Energy Storage," *IEEE Access*, vol. 11, pp. 23245–23259, 2023, doi: 10.1109/ACCESS.2023.3252891.

[4] T. Kerdphol, F. S. Rahman, M. Watanabe, and Y. Mitani, *Virtual Inertia Synthesis and Control*. in Power Systems. Springer International Publishing, 2020. [Online]. Available: https://books.google.com/books?id=UTGjzQEACAAJ

[5] P. Unruh, M. Nuschke, P. Strauss, and F. Welck, "Overview on Grid-Forming Inverter Control Methods," *Energies*, vol. 13, p. 2589, 2020, doi: 10.3390/en13102589.

[6] G. Kryonidis, K.-N. Malamaki, J. M. Mauricio, and C. Demoulias, "A new perspective on the synchronverter model," *Int. J. Electr. Power Energy Syst.*, vol. 140, p. 108072, 2022, doi: 10.1016/j.ijepes.2022.108072.

[7] J. Fang, H. Li, Y. Tang, and F. Blaabjerg, "Distributed Power System Virtual Inertia Implemented by Grid-Connected Power Converters," *IEEE Trans. Power Electron.*, vol. 33, no. 10, pp. 8488–8499, 2018, doi: 10.1109/TPEL.2017.2785218.

[8] L. Huang, H. Xin, H. Yuan, G. Wang, and P. Ju, "Damping Effect of Virtual Synchronous Machines Provided by a Dynamical Virtual Impedance," *IEEE Trans. Energy Convers.*, vol. 36, no. 1, pp. 570–573, 2021, doi: 10.1109/TEC.2020.3040605.

[9] M. Ebrahimi, S. A. Khajehoddin, and M. Karimi-Ghartemani, "An Improved Damping Method for Virtual Synchronous Machines," *IEEE Trans. Sustain. Energy*, vol. 10, no. 3, pp. 1491–1500, 2019, doi: 10.1109/TSTE.2019.2902033.

[10]U. Markovic, N. Früh, P. Aristidou, and G. Hug, "Interval-Based Adaptive Inertia and Damping Control of a Virtual Synchronous Machine," in *2019 IEEE Milan PowerTech*, 2019, pp. 1–6. doi: 10.1109/PTC.2019.8810640.

[11]H. Wu *et al.*, "Small-Signal Modeling and Parameters Design for Virtual Synchronous Generators," *IEEE Trans. Ind. Electron.*, vol. 63, no. 7, pp. 4292–4303, 2016, doi: 10.1109/TIE.2016.2543181.

[12]Q.-C. Zhong and G. Weiss, "Synchronverters: Inverters That Mimic Synchronous Generators," *IEEE Trans. Ind. Electron.*, vol. 58, no. 4, pp. 1259–1267, 2011, doi: 10.1109/TIE.2010.2048839.

[13]V. Natarajan and G. Weiss, "Synchronverters With Better Stability Due to Virtual Inductors, Virtual Capacitors, and Anti-Windup," *IEEE Trans. Ind. Electron.*, vol. 64, no. 7, pp. 5994–6004, 2017, doi: 10.1109/TIE.2017.2674611.

[14]H. Bevrani, B. Francois, and T. Ise, *Microgrid Dynamics and Control*. 2017. doi: 10.1002/9781119263739.

[15]Z. Zhao, Z. Sun, Y. Feng, B. Ji, S. Wang, and J. Zhao, "High-Performance Resonant Controller Implemented in the Discrete-Time Domain for Voltage Regulation of Grid-Forming Converters," *IEEE Trans. Power Electron.*, vol. 37, no. 4, pp. 3913–3926, 2022, doi: 10.1109/TPEL.2021.3120426.

[16]H. Bevrani, *Robust Power System Frequency Control*. 2009. doi: 10.1007/978-0-387-84878-5.

[17]J. Driesen and K. Visscher, "Virtual synchronous generators," in *2008 IEEE Power and Energy Society General Meeting - Conversion and Delivery of Electrical Energy in the 21st Century*, 2008, pp. 1–3. doi: 10.1109/PES.2008.4596800.

[18]J. Liu, Y. Miura, H. Bevrani, and T. Ise, "A Unified Modeling Method of Virtual Synchronous Generator for Multi-Operation-Mode Analyses," *IEEE J. Emerg. Sel. Top. Power Electron.*, vol. 9, no. 2, pp. 2394–2409, 2021, doi: 10.1109/JESTPE.2020.2970025.

[19]H. Bevrani, J. Liu, and T. Kato, "Robust Optimal Damping Control Design For Grid-Forming Converters," in *2021 9th International Renewable and Sustainable Energy Conference (IRSEC)*, 2021, pp. 1–6. doi: 10.1109/IRSEC53969.2021.9741217.

[20]T. Shintai, Y. Miura, and T. Ise, "Oscillation Damping of a Distributed Generator Using a Virtual Synchronous Generator," *IEEE Trans. Power Deliv.*, vol. 29, no. 2, pp. 668–676, 2014, doi: 10.1109/TPWRD.2013.2281359.

[21]L. Huang, H. Xin, and Z. Wang, "Damping Low-Frequency Oscillations Through VSC-HVdc Stations Operated as Virtual Synchronous Machines," *IEEE Trans. Power Electron.*, vol. 34, no. 6, pp. 5803–5818, 2019, doi: 10.1109/TPEL.2018.2866523.

[22]S. Dong and Y. C. Chen, "Adjusting Synchronverter Dynamic Response Speed via Damping Correction Loop," *IEEE Trans. Energy Convers.*, vol. 32, no. 2, pp. 608–619, 2017, doi: 10.1109/TEC.2016.2645450.

[23]J. Liu, Y. Miura, and T. Ise, "A Novel Oscillation Damping Method of Virtual Synchronous Generator Control Without PLL Using Pole Placement," in *2018 International Power Electronics Conference (IPEC-Niigata 2018 -ECCE Asia)*, 2018, pp. 775–781. doi: 10.23919/IPEC.2018.8508003.

[24]J. Liu, Y. Miura, and T. Ise, "Fixed-Parameter Damping Methods of Virtual Synchronous Generator Control Using State Feedback," *IEEE Access*, vol. 7, pp. 99177–99190, 2019, doi: 10.1109/ACCESS.2019.2930132.

[25]F. Blaabjerg, *Control of Power Electronic Converters and Systems Vol 1*. 2018.

[26]J. Liu, Y. Miura, H. Bevrani, and T. Ise, "Enhanced Virtual Synchronous Generator Control for Parallel Inverters in Microgrids," *IEEE Trans. Smart Grid*, vol. 8, no. 5, pp. 2268–2277, 2017, doi: 10.1109/TSG.2016.2521405.

[27]A. Karimi, Y. Jafarian, H. Bevrani, and R. Mirzaei, "Frequency Response Improvement in Microgrids: A Fuzzy–based Virtual Synchronous Generator Approach," *Int. J. Ind. Electron. Control Optim.*, vol. 3, no. 2, pp. 147–158, 2020, [Online]. Available: https://ieco.usb.ac.ir/article_5084.html%0Ahttps://ieco.usb.ac.ir/article_5084_ec47895f67ba5dd947f10ef414763fa1.pdf

[28]M. Li *et al.*, "Phase Feedforward Damping Control Method for Virtual Synchronous Generators," *IEEE Trans. Power*

Electron., vol. 37, no. 8, pp. 9790–9806, 2022, doi: 10.1109/TPEL.2022.3150950.

[29]J. Alipoor, Y. Miura, and T. Ise, "Power System Stabilization Using Virtual Synchronous Generator With Alternating Moment of Inertia," *IEEE J. Emerg. Sel. Top. Power Electron.*, vol. 3, no. 2, pp. 451–458, 2015, doi: 10.1109/JESTPE.2014.2362530.

[30]X. Hou, Y. Sun, X. Zhang, J. Lu, P. Wang, and J. M. Guerrero, "Improvement of Frequency Regulation in VSG-Based AC Microgrid Via Adaptive Virtual Inertia," *IEEE Trans. Power Electron.*, vol. 35, no. 2, pp. 1589–1602, 2020, doi: 10.1109/TPEL.2019.2923734.

[31]M. Li, Y. Wang, N. Xu, W. Wang, and J. Li, "A consistent dynamic response control strategy for virtual synchronous generator," in *2017 IEEE 3rd International Future Energy Electronics Conference and ECCE Asia (IFEEC 2017 - ECCE Asia)*, 2017, pp. 1570–1574. doi: 10.1109/IFEEC.2017.7992280.

[32]D. Li, Q. Zhu, S. Lin, and X. Y. Bian, "A Self-Adaptive Inertia and Damping Combination Control of VSG to Support Frequency Stability," *IEEE Trans. Energy Convers.*, vol. 32, no. 1, pp. 397–398, 2017, doi: 10.1109/TEC.2016.2623982.

[33]M. A. Torres L., L. A. C. Lopes, L. A. Morán T., and J. R. Espinoza C., "Self-Tuning Virtual Synchronous Machine: A Control Strategy for Energy Storage Systems to Support Dynamic Frequency Control," *IEEE Trans. Energy Convers.*, vol. 29, no. 4, pp. 833–840, 2014, doi: 10.1109/TEC.2014.2362577.

[34]S. Qu and Z. Wang, "Cooperative Control Strategy of Virtual Synchronous Generator Based on Optimal Damping Ratio," *IEEE Access*, vol. 9, pp. 709–719, 2021, doi: 10.1109/ACCESS.2020.3046626.

[35]X. Liu *et al.*, "Stability Assessment of A Radial Grid With Power Converters," *IEEE Open J. Power Electron.*, vol. 3, pp. 61–74, 2022, doi: 10.1109/OJPEL.2021.3138509.

[36]M. Li *et al.*, "Unified Modeling and Analysis of Dynamic Power Coupling for Grid-Forming Converters," *IEEE Trans. Power Electron.*, vol. 37, no. 2, pp. 2321–2337, 2022, doi: 10.1109/TPEL.2021.3107329.

[37]L. Harnefors, M. Schweizer, J. Kukkola, M. Routimo, M. Hinkkanen, and X. Wang, "Generic PLL-Based Grid-Forming Control," *IEEE Trans. Power Electron.*, vol. 37, no. 2, pp. 1201–1204, 2022, doi: 10.1109/TPEL.2021.3106045.

[38]Q. Taoufik, E. Rokrok, A. Bruyere, B. Francois, and X. Guillaud, "A PLL-Free Grid-Forming Control With Decoupled Functionalities for High-Power Transmission System Applications," *IEEE Access*, vol. 8, 2020, doi: 10.1109/ACCESS.2020.3034149.

[39]F. Golnaraghi and B. C. Kuo, *Automatic Control Systems*, 10th Editi. New York: McGraw-Hill Education, 2017. [Online]. Available: https://www.accessengineeringlibrary.com/content/book/9781259643835

[40]K. Ogata, *Modern control engineering*. 2010.

[41]O. Kramer, *Genetic Algorithm Essentials*. 2017. doi: 10.1007/978-3-319-52156-5.

[42]S. S. Rao, *Engineering Optimization: Theory and Practice*. Wiley,2019.[Online].Available:https://books.google.nl/books?id=oG21DwAAQBAJ

Anwer J. Ali received his B.E. degree in Electrical Engineering from the Salahaddin University, Hawler, Iraq, in 2000 and his M.Sc. degree in Power Engineering from the University of Sulaimani, Sulaimani, Iraq in 2008. He is currently Ph.D. Student of Control of Power Systems and a member of the Smart/Micro Grids Research Center (SMGRC) at the University of Kurdistan, Sanandaj, Iran. His current research interests include power electronics and virtual dynamics.

Sirwan Shazdeh received PhD degree in electrical engineering from University of Kurdistan (Iran) in 2022. Currently, he is an associate research fellow with Smart/Micro Grids Research Center (SMGRC) at the University of Kurdistan. His current research interests include microgrid dynamics and control, smart grid wide-area protection and control.

Hassan Bevrani (Fellow, IEEE) received the Ph.D. degree in electrical engineering from Osaka University, Osaka, Japan, in 2004. He is currently a Professor and the Program Leader of Smart/Micro Grids Research Center with the University of Kurdistan, Sanandaj, Iran. Over the years, he has worked as a Senior Research Fellow and a Visiting Professor with Osaka University, Kumamoto University, Kyushu Institute of Technology, Doshisha University, Nagoya University (Japan), Queensland University of Technology (Australia), Centrale Lille (France), and Technical University of Berlin (Germany). He is the author and coauthor of 9 international books, 15 book chapters, and more than 500 journal/conference papers. His current research interests include smart grid operation and control, power systems stability and optimization, microgrid dynamics and control, and intelligent/robust control applications in power electric industry.

Rahmatollah Mirzaei received the B.E. degree in electronic engineering from Tabriz University, Tabriz, Iran, in 1987, the M.Sc. degree in control engineering from Tehran University, Tehran, Iran, in 1991, and the Ph.D. degree in the Power Electronics from Indian Institute of Science in Bangalore, India, in 2007. He is currently an Assistant Professor, and a member of the Smart/Micro Grids Research Center at the University of Kurdistan, Sanandaj, Iran, where he was a Lecturer from 1993.

His research interests include design, analysis, control, and modeling of power converters for PFC circuits, soft switching and active filter systems.

Qobad Shafiee (Senior Member, IEEE) received the M.Sc. degree in electrical engineering from the Iran University of Science and Technology, Tehran, Iran, in 2007, and the Ph.D. degree in electrical engineering and microgrids from the Department of Energy Technology, Aalborg Univeristy, Aalborg, Denmark, in 2014. He was with the Department of Electrical and Computer Engineering, University of Kurdistan, Sanandaj, Iran, from 2007 to 2011, where he taught several electrical engineering courses and conducted research on load frequency control of power systems. From March 2014 to June 2014, he was a Visiting Researcher with the Electrical Engineering Department, University of Texas-Arlington, Arlington, TX, USA. He was a Postdoctoral Fellow with the Department of Energy Technology, Aalborg University, in 2015. He is currently an Assistant professor with the Department of Electrical and Computer Engineering, University of Kurdistan. His research interests include modeling, power management, hierarchical and distributed control applied to distributed generation in microgrids.